

SCA-Based Beamforming Optimization for IRS-Enabled Secure Integrated Sensing and Communication

Vaibhav Kumar*, Marwa Chafii^{†‡}, A. Lee Swindlehurst[§], Le-Nam Tran*, and Mark F. Flanagan*

*School of Electrical and Electronic Engineering, University College Dublin, Belfield, Dublin 4, Ireland

[†]Engineering Division, New York University (NYU), Abu Dhabi, UAE

[‡]NYU WIRELESS, NYU Tandon School of Engineering, New York, USA

[§]Center for Pervasive Communications and Computing, University of California, Irvine, CA 92697 USA

Email: vaibhav.kumar@ieee.org, marwa.chafii@nyu.edu, swindle@uci.edu,

nam.tran@ucd.ie, mark.flanagan@ieee.org

Abstract—Integrated sensing and communication (ISAC) is expected to be offered as a fundamental service in the upcoming sixth-generation (6G) communications standard. However, due to the exposure of information-bearing signals to the sensing targets, ISAC poses unique security challenges. In recent years, intelligent reflecting surfaces (IRSs) have emerged as a novel hardware technology capable of enhancing the physical layer security of wireless communication systems. Therefore, in this paper, we consider the problem of transmit and reflective beamforming design in a secure IRS-enabled ISAC system to maximize the beampattern gain at the target. The formulated non-convex optimization problem is challenging to solve due to the intricate coupling between the design variables. Moreover, alternating optimization (AO) based methods are inefficient in finding a solution in such scenarios, and convergence to a stationary point is not theoretically guaranteed. Therefore, we propose a novel successive convex approximation (SCA)-based second-order cone programming (SOCP) scheme in which all of the design variables are updated simultaneously in each iteration. The proposed SCA-based method significantly outperforms a penalty-based benchmark scheme previously proposed in this context. Moreover, we also present a detailed complexity analysis of the proposed scheme, and show that despite having slightly higher per-iteration complexity than the benchmark approach the average problem-solving time of the proposed method is notably lower than that of the benchmark scheme.

Index Terms—Intelligent reflecting surface (IRS), integrated sensing and communication (ISAC), physical layer security, successive convex approximation (SCA), second-order cone programming (SOCP).

I. INTRODUCTION

The sixth-generation (6G) wireless standard is being developed not only to improve the quality of user experience compared to that offered by the fifth-generation networks, but also to support a range of new wireless communication services, such as autonomous vehicles, drone monitoring, human activity recognition, environmental monitoring, enhanced localization and tracking, and many more. Supporting such new services will require the integration of communication, sensing and localization capabilities as fundamental services in a single network architecture rather than as auxiliary functionalities [1]. Integrated sensing and communication (ISAC)

has recently emerged as a potential enabler in this direction, combining the communication and sensing capabilities in a single hardware platform using a common waveform [2], [3]. Preliminary results have confirmed that ISAC can improve the spectral efficiency of a network by virtue of exploiting a common hardware, signal processing and spectral framework, thereby offering a low-cost solution to the spectrum scarcity problem. Furthermore, by exploiting the possibility of communication-centric and sensing-centric designs, it can also enjoy significant coordination gains compared to conventional networks. However, due to the broadcast nature of wireless channels and the inclusion of information-bearing signaling in the sensing waveform, susceptibility to eavesdropping targets poses unique security challenges in ISAC.

Intelligent reflecting surfaces (IRSs) have recently emerged as a groundbreaking hardware technology to robustify wireless communication systems against eavesdroppers via passive beamforming [4]. The benefits of IRS in a secure communication-only multiple-input multiple-output (MIMO) system have been well established in the literature [5], [6]. Hence, it is worth exploring the advantages of IRSs in an ISAC system in terms of physical layer security [7]. However, it is interesting to note that in contrast to the somewhat rich literature on IRS-aided ISAC systems [8]–[12], there is a dearth of literature on *secure* IRS-aided ISAC system design [13], [14]. As one of the few examples, the authors in [13] considered an active IRS-aided multiuser multiple-input single-output (MU-MISO) ISAC system, where the aim was to obtain an optimal beamforming design that maximizes the achievable secrecy rate of the communication users while guaranteeing a minimum radar signal-to-interference-plus-noise ratio (SINR). In [14], the authors considered the problem of beampattern optimization for an eavesdropping target in an IRS-enabled MU-MISO secure ISAC system, subject to SINR constraints at the communication users and information leakage constraints at the target. Two different scenarios were considered in [14]; in the first scenario, full channel state information (CSI) and the target location were assumed to be known at the base station (BS), while imperfect CSI and uncertain target location were assumed in the second scenario. In this paper, we will focus on the first scenario only, where the CSI and target

This work was supported by the Irish Research Council under Grant IRCLA/2017/209, and also in part by Science Foundation Ireland under Grant 17/CDA/4786.

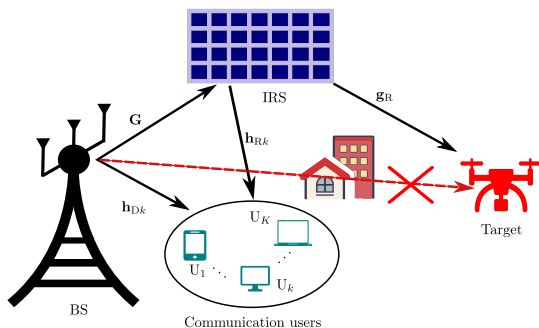


Fig. 1. System model for IRS-enabled secure ISAC system.

location are known at the BS. The more practical setting in which these quantities are imprecisely known will be considered in future work. To optimize the transmit and IRS beamforming in the first scenario, the authors in [14] proposed a penalty-based alternating optimization (AO) algorithm to obtain a semi-closed-form solution using Lagrange duality and a majorization-minimization (MM) algorithm.

Even though the use of AO in [14] makes the optimization problem much easier to solve, it may not produce a high-quality solution because of the complicated interdependence between the design variables [15]. Moreover, as we will show in Section IV, the use of a penalty-based method requires a large number of iterations to achieve convergence and therefore has a very high problem-solving time. Note also that a feasible solution is not guaranteed if the algorithm terminates prematurely. To tackle these issues, in this paper we propose a successive convex approximation (SCA) based beamforming optimization scheme which results in a high-performance solution and also requires a much shorter convergence time. The main contributions of the paper are listed as follows:

- We propose a provably convergent SCA-based algorithm to maximize the beamforming gain at the eavesdropping target in the secure ISAC system, subject to the SINR requirements at the communication users and information leakage constraints at the target. In contrast to the AO-based scheme of [14] where all design variables are updated in an alternating fashion, we derive a second-order cone program (SOCP) where all of the optimization variables are updated *simultaneously* in each iteration.
- We present a complexity analysis of the proposed scheme which demonstrates that the per-iteration complexity grows as $\mathcal{O}(N^{3.5})$, while that of the benchmark solution is given by $\mathcal{O}(N^3)$ [14, Sec. III-C], where N is the number of reflecting elements in the IRS. Although the per-iteration complexity of the proposed approach is slightly higher than that of the benchmark scheme, we show that it requires significantly fewer iterations to converge, resulting in a much shorter problem-solving time.
- We present extensive numerical results to confirm that the proposed SCA-based SOCP approach results in a high-performance solution, and significantly outperforms the

penalty-based AO algorithm in [14].

Notation: Bold uppercase and lowercase letters are used to denote matrices and vectors, respectively. By $\mathbb{C}^{M \times N}$, we denote the vector space of all $M \times N$ complex-valued matrices. By \mathbf{X}^T , \mathbf{X}^H , $\|\mathbf{X}\|$, $\Re\{\mathbf{X}\}$ and $\Im\{\mathbf{X}\}$, we respectively denote the transpose, conjugate transpose, Frobenius norm, real and imaginary components of a matrix \mathbf{X} . $|x|$ denotes the absolute value of a complex number x , and $\text{diag}(x)$ denotes the diagonal matrix whose main diagonal comprises the elements of \mathbf{x} . $\mathcal{O}(\cdot)$ denotes the Bachmann–Landau notation.

II. SYSTEM MODEL AND PROBLEM FORMULATION

Consider the ISAC system shown in Fig. 1 consisting of a multi-antenna dual-function base station (BS), one IRS, K single-antenna communication users (denoted by $U_k, k \in \mathcal{K} \triangleq \{1, 2, \dots, K\}$), and one single-antenna eavesdropping target.¹ Let L and N denote the number of antennas at the BS and the number of elements in the IRS, respectively. We assume that the BS transmits a linear superposition of radar and information signals for the purpose of joint sensing and communication. The signal vector transmitted from the BS is given by

$$\mathbf{s} = \sum_{k \in \mathcal{K}} \mathbf{x}_k w_k + \sum_{l \in \mathcal{L}} \hat{\mathbf{x}}_l \hat{w}_l, \quad (1)$$

where w_k is the communication signal intended for U_k and \hat{w}_l is the l^{th} radar signal with $l \in \mathcal{L} \triangleq \{1, 2, \dots, L\}$. Moreover, $\mathbf{x}_k \in \mathbb{C}^{L \times 1}$ and $\hat{\mathbf{x}}_l \in \mathbb{C}^{L \times 1}$ are the beamforming vectors corresponding to w_k and \hat{w}_l , respectively. It is assumed that $\mathbb{E}\{w_k\} = 0$, $\mathbb{E}\{|w_k|^2\} = 1 \forall k \in \mathcal{K}$, $\mathbb{E}\{\hat{w}_l\} = 0$, $\mathbb{E}\{|\hat{w}_l|^2\} = 1 \forall l \in \mathcal{L}$, and $\mathbb{E}\{w_k \hat{w}_l^H\} = 0 \forall k \in \mathcal{K}, l \in \mathcal{L}$, i.e., the communication and radar signals are mutually independent and uncorrelated. Denoting the BS-IRS, BS- U_k and IRS- U_k links by $\mathbf{G} \in \mathbb{C}^{N \times L}$, $\mathbf{h}_{Dk} \in \mathbb{C}^{1 \times L}$, and $\mathbf{h}_{Rk} \in \mathbb{C}^{1 \times N}$, respectively, the signal received at U_k is given by

$$y_k = \mathbf{h}_k \mathbf{s} + z_k, \quad (2)$$

where $\mathbf{h}_k \triangleq \mathbf{h}_{Dk} + \mathbf{h}_{Rk} \Theta \mathbf{G}$, $\Theta \triangleq \text{diag}(\boldsymbol{\theta})$, $\boldsymbol{\theta} = [\theta_1, \theta_2, \dots, \theta_N]^T$, $\theta_n \triangleq \exp(j2\pi\phi_n)$ with $\phi_n \in [0, 2\pi)$ denoting the phase shift induced by the n^{th} IRS element, and z_k denotes the zero-mean complex additive white Gaussian noise (AWGN) at U_k with variance σ_k^2 .

Defining $\mathbf{X} \triangleq [\mathbf{x}_1, \mathbf{x}_2, \dots, \mathbf{x}_K, \hat{\mathbf{x}}_1, \hat{\mathbf{x}}_2, \dots, \hat{\mathbf{x}}_L] \in \mathbb{C}^{L \times (K+L)}$, and $\tilde{\mathbf{x}}_m$ as the m^{th} column of \mathbf{X} , the signal-to-interference-plus-noise ratio (SINR) at U_k to decode the intended message is given by

$$\gamma_k = \frac{|\mathbf{h}_k \mathbf{x}_k|^2}{\sigma_k^2 + \sum_{\ell \in \mathcal{M} \setminus \{k\}} |\mathbf{h}_k \tilde{\mathbf{x}}_\ell|^2}, \quad (3)$$

where $\mathcal{M} \triangleq \{1, 2, \dots, K, K+1, \dots, K+L\}$. Similarly, by denoting the IRS-target channel by $\mathbf{g}_R \in \mathbb{C}^{1 \times N}$ and assuming that the BS-target (direct) link is blocked due to obstacles, the signal received at the target is given by

$$y_T = \mathbf{g}_T \mathbf{s} + z_T, \quad (4)$$

¹Although we consider a single eavesdropping target in this paper, it is straightforward to use the proposed algorithm for a system with multiple eavesdropping targets.

where $\mathbf{g} \triangleq \mathbf{g}_R \Theta \mathbf{G} \in \mathbb{C}^{1 \times L}$, \mathbf{g}_R is the steering vector from the IRS in the direction of the target, and z_T is the zero-mean complex AWGN at the target with variance σ_T^2 . Therefore, the SINR at the target to wiretap the signal intended for U_k is given by

$$\hat{\gamma}_k = \frac{|\mathbf{g} \mathbf{x}_k|^2}{\sigma_T^2 + \sum_{\ell \in \mathcal{M} \setminus \{k\}} |\mathbf{g} \tilde{\mathbf{x}}_\ell|^2}. \quad (5)$$

We assume that all of the channels and the target location are perfectly known to the BS. The beampattern gain toward the target is then given by (c.f. [14])

$$\mathcal{G}(\mathbf{X}, \boldsymbol{\theta}) = \mathbb{E}\{|\mathbf{g} \mathbf{s}|^2\} = \sum_{m \in \mathcal{M}} |\mathbf{g} \tilde{\mathbf{x}}_m|^2. \quad (6)$$

Therefore, the problem of maximizing the beampattern gain toward the target is given by

$$\underset{\mathbf{X}, \boldsymbol{\theta}}{\text{maximize}} \mathcal{G}(\mathbf{X}, \boldsymbol{\theta}), \quad (7a)$$

$$\text{subject to } \gamma_k \geq \Gamma_k \quad \forall k \in \mathcal{K}, \quad (7b)$$

$$\hat{\gamma}_k \leq \hat{\Gamma}_k \quad \forall k \in \mathcal{K}, \quad (7c)$$

$$\|\mathbf{X}\| \leq \sqrt{P} \quad (7d)$$

$$|\theta_n|^2 = 1 \quad \forall n \in \mathcal{N} \triangleq \{1, 2, \dots, N\}, \quad (7e)$$

where (7b) ensures that the SINR at U_k is greater than or equal to the predefined threshold Γ_k , (7c) enforces the constraint that the maximum leakage of the information intended for U_k at the eavesdropping target is below the tolerance level $\hat{\Gamma}_k$ and P is the transmit power budget at the BS. Note that in a system with heterogeneous secrecy requirements, considering information leakage constraints results in a more flexible resource allocation compared to that offered via imposing constraints on the achievable secrecy rate [16]. It is easy to note that due to coupling between the design variables \mathbf{X} and $\boldsymbol{\theta}$ in (7a)–(7c) and the non-convex constraints in (7e), the problem in (7) is non-convex and challenging to solve.

Hua *et al.* [14] proposed a penalty-based dual-loop AO algorithm to obtain a solution to (7). More specifically, in the inner loop, auxiliary variables were updated by solving a quadratically-constrained quadratic program (QCQP), the beamformers (i.e., \mathbf{X}) were updated using a bisection search, and the IRS reflection coefficients ($\boldsymbol{\theta}$) were updated via MM; the outer loop was used to update the penalty parameter only. Although the use of auxiliary variables and the penalty method in [14] resulted in a reformulated optimization problem where the design variables were decoupled in the constraints, obtaining a high quality solution is not guaranteed via AO. Additionally, although the per-iteration complexity of the penalty-based solution in [14] was $\mathcal{O}(N^3)$, because of the use of bisection search and the dual-loop structure, the number of iterations required for convergence is large. This in turn results in a high problem-solving time because if the iterations are terminated prematurely (i.e., before the penalty terms becomes nearly zero), the obtained solution may not be feasible.

III. PROPOSED SOLUTION

In this section, we apply a series of convex approximations to tackle the non-convexity of (7) and to obtain a high-performance solution. In this regard, for two arbitrary complex-valued vectors \mathbf{u} and \mathbf{v} , we recall the following (in)equalities (c.f. [17, eqn. (6)])

$$\|\mathbf{u}\|^2 \geq 2\Re\{\mathbf{v}^H \mathbf{u}\} - \|\mathbf{v}\|^2, \quad (8a)$$

$$\Re\{\mathbf{u}^H \mathbf{v}\} = \frac{1}{4}(\|\mathbf{u} + \mathbf{v}\|^2 - \|\mathbf{u} - \mathbf{v}\|^2), \quad (8b)$$

$$\Im\{\mathbf{u}^H \mathbf{v}\} = \frac{1}{4}(\|\mathbf{u} - j\mathbf{v}\|^2 - \|\mathbf{u} + j\mathbf{v}\|^2). \quad (8c)$$

Next, we note that the term in (7a) is neither convex nor concave. Since we want to maximize the function in (7a), we obtain a corresponding *concave lower bound* as follows:

$$\begin{aligned} \mathcal{G}(\mathbf{X}, \boldsymbol{\theta}) &= \sum_{m \in \mathcal{M}} |\mathbf{g} \tilde{\mathbf{x}}_m|^2 \\ &\stackrel{(a)}{\geq} \sum_{m \in \mathcal{M}} [2\Re\{a_m^{(i)H} \mathbf{g} \tilde{\mathbf{x}}_m\} - |a_m^{(i)}|^2] \\ &\stackrel{(b)}{=} \sum_{m \in \mathcal{M}} \left[\frac{1}{2} \{ \|a_m^{(i)} \mathbf{g}^H + \tilde{\mathbf{x}}_m\|^2 - \|a_m^{(i)} \mathbf{g}^H - \tilde{\mathbf{x}}_m\|^2 \} - |a_m^{(i)}|^2 \right] \\ &\stackrel{(c)}{\geq} \sum_{m \in \mathcal{M}} \left[\Re\{\mathbf{b}_m^{(i)H} [a_m^{(i)} \mathbf{g}^H + \tilde{\mathbf{x}}_m]\} - \frac{1}{2} \|\mathbf{b}_m^{(i)}\|^2 \right. \\ &\quad \left. - \frac{1}{2} \|a_m^{(i)} \mathbf{g}^H - \tilde{\mathbf{x}}_m\|^2 - |a_m^{(i)}|^2 \right] \\ &\triangleq \sum_{m \in \mathcal{M}} f_m(\tilde{\mathbf{x}}_m, \boldsymbol{\theta}; \tilde{\mathbf{x}}_m^{(i)}, \boldsymbol{\theta}^{(i)}), \end{aligned} \quad (9)$$

where $\tilde{\mathbf{x}}_m^{(i)}$ and $\boldsymbol{\theta}^{(i)}$ denote the value of $\tilde{\mathbf{x}}_m$ and $\boldsymbol{\theta}$ in the i^{th} iteration of the SCA process, respectively. Moreover, (a) and (c) follow from (8a), and (b) follows from (8b). Additionally in (9), $a_m^{(i)} \triangleq \mathbf{g}^{(i)} \tilde{\mathbf{x}}_m^{(i)}$, $\mathbf{b}_m^{(i)} \triangleq a_m^{(i)} \mathbf{g}^{(i)H} + \tilde{\mathbf{x}}_m^{(i)}$, and $\mathbf{g}^{(i)} \triangleq \mathbf{g}_R \Theta^{(i)} \mathbf{G}$. Note that $f_m(\tilde{\mathbf{x}}_m, \boldsymbol{\theta}; \tilde{\mathbf{x}}_m^{(i)}, \boldsymbol{\theta}^{(i)})$ is *jointly concave* with respect to (w.r.t.) $\tilde{\mathbf{x}}_m$ and $\boldsymbol{\theta}$.

Next, we turn our attention to the non-convex constraints in (7b). Using (3), for any $k \in \mathcal{K}$, we can equivalently represent (7b) as follows:

$$\frac{1}{\Gamma_k} |\mathbf{h}_k \mathbf{x}_k|^2 \geq \sigma_k^2 + \sum_{\ell \in \mathcal{M} \setminus \{k\}} (\varphi_{k\ell}^2 + \bar{\varphi}_{k\ell}^2), \quad (10a)$$

$$\varphi_{k\ell} \geq |\Re\{\mathbf{h}_k \tilde{\mathbf{x}}_\ell\}| \quad \forall \ell \in \mathcal{M} \setminus \{k\}, \quad (10b)$$

$$\bar{\varphi}_{k\ell} \geq |\Im\{\mathbf{h}_k \tilde{\mathbf{x}}_\ell\}| \quad \forall \ell \in \mathcal{M} \setminus \{k\}. \quad (10c)$$

It is easy to see that if (7b) is feasible, then so is (10) and vice versa. Note that the right-hand side (RHS) of (10a) is convex, and we only need to obtain a concave lower bound on the left-hand side (LHS) of (10a). Following a similar line of argument to (9), this can be done as follows:

$$\begin{aligned} \frac{1}{\Gamma_k} |\mathbf{h}_k \mathbf{x}_k|^2 &\geq \frac{1}{\Gamma_k} \Re\{(\mathbf{d}_k^{(i)H}) [c_k^{(i)} \mathbf{h}_k^H + \mathbf{x}_k]\} - \frac{1}{2} \|\mathbf{d}_k^{(i)}\|^2 \\ &\quad - \frac{1}{2} \|c_k^{(i)} \mathbf{h}_k^H - \mathbf{x}_k\|^2 - |c_k^{(i)}|^2 \triangleq \frac{1}{\Gamma_k} \bar{f}_k(\mathbf{x}_k, \boldsymbol{\theta}; \mathbf{x}_k^{(i)}, \boldsymbol{\theta}^{(i)}), \end{aligned} \quad (11)$$

where $c_k^{(i)} \triangleq \mathbf{h}_k^{(i)} \mathbf{x}_k^{(i)}$ and $\mathbf{d}_k^{(i)} \triangleq c_k^{(i)} \mathbf{h}_k^{(i)H} + \mathbf{x}_k^{(i)}$.

Using the fact that $u \geq |v|$ iff $u \geq v$ or $u \geq -v$, and following (8b), $\wp_{k\ell}$ in (10b) can be equivalently written as

$$\wp_{k\ell} \geq \Re\{\mathbf{h}_k \tilde{\mathbf{x}}_\ell\} = \frac{1}{4}(\|\mathbf{h}_k^H + \tilde{\mathbf{x}}_\ell\|^2 - \|\mathbf{h}_k^H - \tilde{\mathbf{x}}_\ell\|^2), \quad (12a)$$

$$\wp_{k\ell} \geq -\Re\{\mathbf{h}_k \tilde{\mathbf{x}}_\ell\} = \frac{1}{4}(\|\mathbf{h}_k^H - \tilde{\mathbf{x}}_\ell\|^2 - \|\mathbf{h}_k^H + \tilde{\mathbf{x}}_\ell\|^2). \quad (12b)$$

Since the negative quadratic term in the RHS of (12a) results in its non-convexity, we use the inequality in (8a) to convexify (12a) as follows:

$$\wp_{k\ell} \geq \frac{1}{4}[\|\mathbf{h}_k^H + \tilde{\mathbf{x}}_\ell\|^2 - 2\Re\{(\mathbf{h}_k^{(i)} - \tilde{\mathbf{x}}_\ell^{(i)H})(\mathbf{h}_k^H - \tilde{\mathbf{x}}_\ell)\} + \|\mathbf{h}_k^{(i)H} - \tilde{\mathbf{x}}_\ell^{(i)}\|^2] \triangleq \mu_{k\ell}(\tilde{\mathbf{x}}_\ell, \boldsymbol{\theta}; \tilde{\mathbf{x}}_\ell^{(i)}, \boldsymbol{\theta}^{(i)}). \quad (13)$$

Following a similar argument, (12b) yields

$$\wp_{k\ell} \geq \frac{1}{4}[\|\mathbf{h}_k^H - \tilde{\mathbf{x}}_\ell\|^2 - 2\Re\{(\mathbf{h}_k^{(i)} + \tilde{\mathbf{x}}_\ell^{(i)H})(\mathbf{h}_k^H + \tilde{\mathbf{x}}_\ell)\} + \|\mathbf{h}_k^{(i)H} + \tilde{\mathbf{x}}_\ell^{(i)}\|^2] \triangleq \bar{\mu}_{k\ell}(\tilde{\mathbf{x}}_\ell, \boldsymbol{\theta}; \tilde{\mathbf{x}}_\ell^{(i)}, \boldsymbol{\theta}^{(i)}). \quad (14)$$

Analogously, (10c) yields the following inequalities:

$$\bar{\wp}_{k\ell} \geq \frac{1}{4}[\|\mathbf{h}_k^H - j\tilde{\mathbf{x}}_\ell\|^2 - 2\Re\{(\mathbf{h}_k^{(i)} - j\tilde{\mathbf{x}}_\ell^{(i)H})(\mathbf{h}_k^H + j\tilde{\mathbf{x}}_\ell)\} + \|\mathbf{h}_k^{(i)H} + j\tilde{\mathbf{x}}_\ell^{(i)}\|^2] \triangleq v_{k\ell}(\tilde{\mathbf{x}}_\ell, \boldsymbol{\theta}; \tilde{\mathbf{x}}_\ell^{(i)}, \boldsymbol{\theta}^{(i)}), \quad (15)$$

$$\bar{\wp}_{k\ell} \geq \frac{1}{4}[\|\mathbf{h}_k^H + j\tilde{\mathbf{x}}_\ell\|^2 - 2\Re\{(\mathbf{h}_k^{(i)} + j\tilde{\mathbf{x}}_\ell^{(i)H})(\mathbf{h}_k^H - j\tilde{\mathbf{x}}_\ell)\} + \|\mathbf{h}_k^{(i)H} - j\tilde{\mathbf{x}}_\ell^{(i)}\|^2] \triangleq \bar{v}_{k\ell}(\tilde{\mathbf{x}}_\ell, \boldsymbol{\theta}; \tilde{\mathbf{x}}_\ell^{(i)}, \boldsymbol{\theta}^{(i)}). \quad (16)$$

We now focus on the non-convex constraint in (7c), which for any $k \in \mathcal{K}$, can be written as

$$\hat{\gamma}_k \leq \hat{\Gamma}_k \Rightarrow \sigma_{\hat{\Gamma}}^2 + \sum_{\ell \in \mathcal{M} \setminus \{k\}} |\mathbf{g}\tilde{\mathbf{x}}_\ell|^2 \geq \frac{1}{\hat{\Gamma}} |\mathbf{g}\mathbf{x}_k|^2. \quad (17)$$

Note that we need a *concave lower bound* on the LHS of (17), and a *convex upper bound* on the RHS. Similar to (9), the former can be obtained by linearizing the quadratic term in the LHS as follows:

$$\sigma_{\hat{\Gamma}}^2 + \sum_{\ell \in \mathcal{M} \setminus \{k\}} |\mathbf{g}\tilde{\mathbf{x}}_\ell|^2 \geq \sigma_{\hat{\Gamma}}^2 + \sum_{\ell \in \mathcal{M} \setminus \{k\}} f_\ell(\tilde{\mathbf{x}}_\ell, \boldsymbol{\theta}; \tilde{\mathbf{x}}_\ell^{(i)}, \boldsymbol{\theta}^{(i)}). \quad (18)$$

On the other hand, a convex upper bound on $|\mathbf{g}\mathbf{x}_k|^2/\hat{\Gamma}$ is given by $(\tau_k^2 + \bar{\tau}_k^2)/\hat{\Gamma}$, where $\tau_k \geq |\Re\{\mathbf{g}\mathbf{x}_k\}|$ and $\bar{\tau}_k \geq |\Im\{\mathbf{g}\mathbf{x}_k\}|$. Therefore, using (17), (18) and the preceding arguments, for a given $k \in \mathcal{K}$, the constraint in (7c) can be equivalently written as

$$\sigma_{\hat{\Gamma}}^2 + \sum_{\ell \in \mathcal{M} \setminus \{k\}} f_\ell(\tilde{\mathbf{x}}_\ell, \boldsymbol{\theta}; \tilde{\mathbf{x}}_\ell^{(i)}, \boldsymbol{\theta}^{(i)}) \geq \frac{1}{\hat{\Gamma}_k} (\tau_k^2 + \bar{\tau}_k^2), \quad (19a)$$

$$\tau_k \geq |\Re\{\mathbf{g}\mathbf{x}_k\}|, \quad (19b)$$

$$\bar{\tau}_k \geq |\Im\{\mathbf{g}\mathbf{x}_k\}|. \quad (19c)$$

Again, it can be noted that if (7c) is feasible, then so is (19) and vice versa. Moreover, following a similar set of arguments to those in (12)–(16), lower bounds on τ_k and $\bar{\tau}_k$ in (19b) and (19c), respectively, are given by

$$\tau_k \geq \frac{1}{4}[\|\mathbf{g}^H + \mathbf{x}_k\|^2 - 2\Re\{(\mathbf{g}^{(i)} - \mathbf{x}_k^{(i)H})(\mathbf{g}^H - \mathbf{x}_k)\}]$$

Algorithm 1: Proposed SCA-based Method to Solve (21).

Input: $\mathbf{X}^{(0)}$, $\boldsymbol{\theta}^{(0)}$, $\xi > 0$

1 $i \leftarrow 0$;

2 **repeat**

3 Solve (21) and denote the solution as \mathbf{X}^* , $\boldsymbol{\theta}^*$;

4 Update: $\mathbf{X}^{(i+1)} \leftarrow \mathbf{X}^*$, $\boldsymbol{\theta}^{(i+1)} \leftarrow \boldsymbol{\theta}^*$;

5 $i \leftarrow i + 1$;

6 **until** convergence;

Output: \mathbf{X}^* , $\boldsymbol{\theta}^*$

$$+ \|\mathbf{g}^{(i)H} - \mathbf{x}_k^{(i)}\|^2] \triangleq \eta_k(\mathbf{x}_k, \boldsymbol{\theta}; \mathbf{x}_k^{(i)}, \boldsymbol{\theta}^{(i)}), \quad (20a)$$

$$\tau_k \geq \frac{1}{4}[\|\mathbf{g}^H - \mathbf{x}_k\|^2 - 2\Re\{(\mathbf{g}^{(i)} + \mathbf{x}_k^{(i)H})(\mathbf{g}^H + \mathbf{x}_k)\} + \|\mathbf{g}^{(i)H} + \mathbf{x}_k^{(i)}\|^2] \triangleq \bar{\eta}_k(\mathbf{x}_k, \boldsymbol{\theta}; \mathbf{x}_k^{(i)}, \boldsymbol{\theta}^{(i)}), \quad (20b)$$

$$\bar{\tau}_k \geq \frac{1}{4}[\|\mathbf{g}^H - j\mathbf{x}_k\|^2 - 2\Re\{(\mathbf{g}^{(i)} - j\mathbf{x}_k^{(i)H})(\mathbf{g}^H + j\mathbf{x}_k)\} + \|\mathbf{g}^{(i)H} + j\mathbf{x}_k^{(i)}\|^2] \triangleq \chi_k(\mathbf{x}_k, \boldsymbol{\theta}; \mathbf{x}_k^{(i)}, \boldsymbol{\theta}^{(i)}), \quad (20c)$$

$$\bar{\tau}_k \geq \frac{1}{4}[\|\mathbf{g}^H + j\mathbf{x}_k\|^2 - 2\Re\{(\mathbf{g}^{(i)} + j\mathbf{x}_k^{(i)H})(\mathbf{g}^H - j\mathbf{x}_k)\} + \|\mathbf{g}^{(i)H} - j\mathbf{x}_k^{(i)}\|^2] \triangleq \bar{\chi}_k(\mathbf{x}_k, \boldsymbol{\theta}; \mathbf{x}_k^{(i)}, \boldsymbol{\theta}^{(i)}). \quad (20d)$$

Next, since the constraint in (7d) is already convex, we are left only with the non-convexity of (7e). To tackle this, we first relax the equality constraint in (7e) by a (convex) inequality constraint. In order to ensure that the inequality constraint is satisfied with equality (i.e., the constraint is binding at convergence), we add a regularization term in the objective and handle the resulting non-convex objective by the first-order approximation of the regularization term around $\boldsymbol{\theta}^{(i)}$. Therefore, an equivalent reformulation of the problem in (7) can be given by

$$\begin{aligned} & \underset{\mathbf{X}, \boldsymbol{\theta}, \wp, \bar{\wp}, \tau, \bar{\tau}}{\text{maximize}} \quad \sum_{m \in \mathcal{M}} f_m(\tilde{\mathbf{x}}_m, \boldsymbol{\theta}; \tilde{\mathbf{x}}_m^{(i)}, \boldsymbol{\theta}^{(i)}) \\ & \quad + \zeta [2\Re\{\boldsymbol{\theta}^{(n)H} \boldsymbol{\theta}\} - \|\boldsymbol{\theta}^{(n)}\|^2], \end{aligned} \quad (21a)$$

$$\begin{aligned} & \text{subject to} \quad \frac{1}{\hat{\Gamma}_k} \bar{f}_k(\mathbf{x}_k, \boldsymbol{\theta}; \mathbf{x}_k^{(i)}, \boldsymbol{\theta}^{(i)}) \\ & \quad \geq \sigma_k^2 + \sum_{\ell \in \mathcal{M} \setminus \{k\}} (\wp_{k\ell}^2 + \bar{\wp}_{k\ell}^2) \quad \forall k \in \mathcal{K}, \end{aligned} \quad (21b)$$

$$(13) - (16) \quad \forall k \in \mathcal{K}, \forall \ell \in \mathcal{M} \setminus \{k\}, \quad (21c)$$

$$(19a), (20) \quad \forall k \in \mathcal{K},$$

$$(7d),$$

$$|\theta_n| \leq 1 \quad \forall n \in \mathcal{N}, \quad (21d)$$

where $\wp \triangleq [\wp_{11}, \wp_{12}, \dots, \wp_{KL}]^T$, $\bar{\wp} \triangleq [\bar{\wp}_{11}, \bar{\wp}_{12}, \dots, \bar{\wp}_{KL}]^T$, $\tau \triangleq [\tau_1, \tau_2, \dots, \tau_K]^T$, $\bar{\tau} \triangleq [\bar{\tau}_1, \bar{\tau}_2, \dots, \bar{\tau}_K]^T$, and $\zeta > 0$ is the regularization parameter. It is straightforward to show that all of the constraints in (21) can be represented by quadratic cones, and therefore (21) is an SOCP problem which can be solved efficiently using off-the-shelf solvers, e.g., MOSEK [18]. The proposed SCA-based SOCP method is outlined in **Algorithm 1**.

Remark 1. One needs to find feasible starting points $\mathbf{X}^{(0)}$ and $\boldsymbol{\theta}^{(0)}$ to run **Algorithm 1**, which is not straightforward. Therefore, below we describe a practical way to obtain a set of initial points. Consider the following optimization problem:

$$\underset{\mathbf{X}, \boldsymbol{\theta}, \boldsymbol{\delta}, \bar{\boldsymbol{\delta}}}{\text{minimize}} \quad \sum_{k \in \mathcal{K}} (\delta_k + \bar{\delta}_k), \quad (22a)$$

$$\begin{aligned} \text{subject to} \quad & \delta_k + \frac{1}{\Gamma_k} \bar{f}_k(\mathbf{x}_k, \boldsymbol{\theta}; \mathbf{x}_k^{(i)}, \boldsymbol{\theta}^{(i)}) \\ & \geq \sigma_k^2 + \sum_{\ell \in \mathcal{M} \setminus \{k\}} (\varphi_{k\ell}^2 + \bar{\varphi}_{k\ell}^2) \quad \forall k \in \mathcal{K}, \end{aligned} \quad (22b)$$

$$\begin{aligned} & \bar{\delta}_k + \sigma_T^2 + \sum_{\ell \in \mathcal{M} \setminus \{k\}} f_\ell(\tilde{\mathbf{x}}_\ell, \boldsymbol{\theta}; \tilde{\mathbf{x}}_\ell^{(i)}, \boldsymbol{\theta}^{(i)}) \\ & \geq \frac{1}{\bar{\Gamma}_k} (\tau_k^2 + \bar{\tau}_k^2) \quad \forall k \in \mathcal{K}, \end{aligned} \quad (22c)$$

$$(7d), (7e), (20), (21c),$$

$$\delta_k \geq 0, \bar{\delta}_k \geq 0 \quad \forall k \in \mathcal{K}. \quad (22d)$$

Note that the problem in (22) is always feasible for sufficiently large $\boldsymbol{\delta}$ and $\bar{\boldsymbol{\delta}}$. We solve the problem in (22) by following a similar procedure to that of **Algorithm 1**, with random \mathbf{X} and $\boldsymbol{\theta}$ as initial points. The minimization in 22 forces δ_k and $\bar{\delta}_k$ to approach 0. At convergence, if $\delta_k = \bar{\delta}_k = 0 \quad \forall k \in \mathcal{K}$, the problem in (21) is obviously feasible. Thus we can choose the final values of \mathbf{X} and $\boldsymbol{\theta}$ in (22) as initial points for **Algorithm 1**. However, if the objective $\sum_{k \in \mathcal{K}} (\delta_k + \bar{\delta}_k)$ is not zero at convergence, then we simply declare that the considered problem is infeasible and will not run **Algorithm 1**²

The convergence of the proposed SCA-based method in **Algorithm 1** can be readily proved following the set of arguments in [17, Sec. III-A].

A. Complexity Analysis

It is straightforward to show that the total number of (real-valued) optimization variables in (21) is $2(L^2 + K^2 + 2KL + N) + 1$, and the total number of (second-order) conic constraints is $4K^2 + 4KL + 2K + N + 2$. Therefore, following the arguments in [19, Sec. 6.6.2], the overall per-iteration complexity of the proposed SOCP-based method is given by

$$\begin{aligned} & \mathcal{O}[(4K^2 + 4KL + N)^{0.5} (2K^2 + 4KL + 2L^2 + 2N) \\ & (4K^5 + 8K^4L + 4K^3L^2 + 48K^3L + 60K^2L^2 + 24KL^3 \\ & + 52KL^2 + 4L^4 + (2K^2 + 4KL + 2L^2 + 2N)^2)]. \end{aligned} \quad (23)$$

However, in a practical setup, the number of elements in the IRS is expected to be much larger than the number of BS antennas and the number of users, i.e., $N \gg \max\{L, K\}$. Hence, the complexity of the proposed SCA-based method can be well-approximated by $\mathcal{O}(N^{3.5})$. On the other hand, the per-iteration computational complexity of [14, Algorithm 1] can

²We note that the considered problem may be feasible even though $\sum_{k \in \mathcal{K}} (\delta_k + \bar{\delta}_k) > 0$. The reason is that the SCA-based method applied to solve (22) can only guarantee a stationary solution. In general, checking (7) is feasible or not is an NP hard problem since the feasible set is non-convex. For practical purposes, if the SCA-based method cannot find a feasible solution, we can simply say that the problem is infeasible and ignore this realization.

be approximated by $\mathcal{O}(N^3)$ (see [14, Sec. III-C]). Although the order of complexity of the proposed SCA-based method is slightly higher than that of the penalty-based benchmark, we will show in the simulation section that the proposed method requires fewer iterations, resulting in a significantly reduced problem-solving time.

IV. NUMERICAL RESULTS AND DISCUSSION

In this section, we present a detailed performance comparison between the proposed SCA-based method and the penalty-based benchmark approach of [14, Algorithm 1]. The location of the nodes and the channel model assumed here are the same as those in [14]. The simulations are performed on a high-performance computing cluster with a Intel Xeon Gold 6152 processor, using Python v3.9.7 and MOSEK Fusion API for Python Rel.-10.0.40 [18]. In Figs. 3 and 4, the results are obtained by averaging over 100 independent channel realizations.

In Fig. 2, we show the convergence behavior of both the proposed and penalty-based benchmark methods. For the given set of channels, the proposed SCA-based method converges in less than 30 iterations, whereas the penalty-based benchmark requires around 270 iterations. Nevertheless, even with significantly fewer iterations, the proposed method results in nearly a 30% higher beampattern gain as compared to that offered by the penalty-based benchmark. More interestingly, each iteration of the proposed SCA-based method returns a set of feasible points and therefore the iterations of the proposed method can be terminated even before convergence has been attained, if this is required. On the other hand, the penalty-based benchmark returns a feasible solution only in the final outer-loop iteration, and therefore the algorithm cannot be stopped earlier to achieve a feasible solution. Therefore, the benchmark is not suitable in rapidly changing environments with very small coherence times where at least a suboptimal solution is required within a certain fraction of the channel's coherence time.

The impact of the number of IRS elements on the average beampattern gain for the two algorithms- is shown in Fig. 3. An increase in the number of IRS elements increases the degrees-of-freedom at the IRS, allowing the IRS to perform highly focused beamforming. This in turn results in increasing beampattern gain with increasing N . On the other hand, since a fixed amount of transmit power is required to achieve the SINR constraints at the communication users, a higher transmit power budget results in a higher surplus power at the BS, which is then used to attain a larger beampattern gain toward the target. Therefore, increasing the value of P increases the average beampattern gain, which is also clearly evident from the figure. The performance gap between the SCA-based and penalty-based methods increases with an increase in the number of IRS elements. As the value of N increases, the impact of coupling between \mathbf{X} and $\boldsymbol{\theta}$ becomes more intricate. Therefore, the solution obtained via the AO-based approach of [14] returns a highly suboptimal beampattern gain. On the other hand, as clearly observed in the figure, the simultaneous

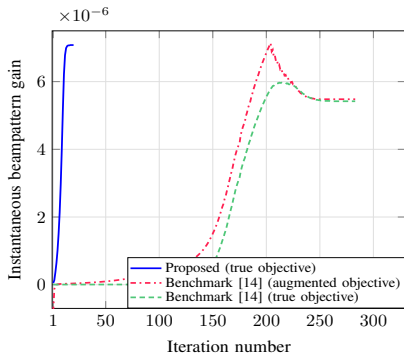


Fig. 2. Convergence results for $L = 4$, $K = 3$, $N = 100$, $P = 40$ dBm, $\Gamma_k = 10$ dB $\forall k \in \mathcal{K}$ and $\hat{\Gamma}_k = 0$ dB $\forall k \in \mathcal{K}$.

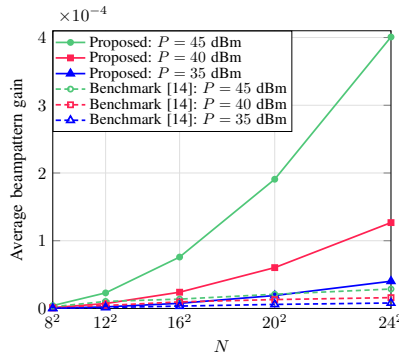


Fig. 3. Average beampattern gain for $L = 4$, $K = 3$, $\Gamma_k = 10$ dB $\forall k \in \mathcal{K}$ and $\hat{\Gamma}_k = 0$ dB $\forall k \in \mathcal{K}$.

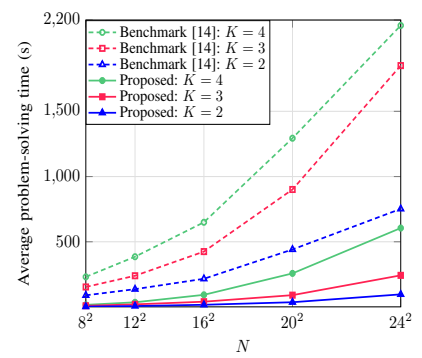


Fig. 4. Average problem solving time for $L = 4$, $P = 40$ dBm, $\Gamma_k = 10$ dB $\forall k \in \mathcal{K}$ and $\hat{\Gamma}_k = 0$ dB $\forall k \in \mathcal{K}$.

update of all variables in the proposed algorithm outperforms the penalty-based benchmark.

In Fig. 4, we plot the average problem-solving time versus the number of IRS elements for different numbers of communication users K . As the value of N and/or K increases, the size of the optimization problem to be solved also increases for both methods. This in turn increases the average problem solving time for both approaches. Although the per-iteration complexity of the proposed SCA-based method is slightly higher than that of the penalty-based benchmark, the proposed approach requires a much smaller time to find the solution due to its convergence in fewer iterations.

V. CONCLUSION

In this paper, we have considered the problem of optimal transmit and reflective beamforming design in a secure IRS-enabled ISAC system. More specifically, we aim to maximize the beampattern gain toward the eavesdropping target subject to the SINR constraints at the communication users and information leakage constraints at the target. In contrast to the conventional AO-based approach, we proposed a novel SCA-based optimization in which all variables are updated simultaneously. The superiority of the proposed method was clearly established with the help of numerical experiments in terms of both achieving a high-performance solution and low problem-solving time compared to that of the penalty-based benchmark. Moreover, the performance gap between the proposed SCA-based approach and penalty-based benchmark was shown to be increasing with the number of IRS elements or the transmit power budget.

REFERENCES

- [1] Z. Wei, F. Liu, C. Masouros, N. Su, and A. P. Petropulu, "Toward multifunctional 6G wireless networks: Integrating sensing, communication, and security," *IEEE Commun. Mag.*, vol. 60, no. 4, pp. 65–71, 2022.
- [2] D. Ma, N. Shlezinger, T. Huang, Y. Liu, and Y. C. Eldar, "Joint radar-communication strategies for autonomous vehicles: Combining two key automotive technologies," *IEEE Signal Process. Mag.*, vol. 37, no. 4, pp. 85–97, 2020.

- [3] X. Fang, W. Feng, Y. Chen, N. Ge, and Y. Zhang, "Joint communication and sensing toward 6G: Models and potential of using MIMO," *IEEE Internet Things J.*, vol. 10, no. 5, pp. 4093–4116, 2023.
- [4] Z. Chen *et al.*, "Reconfigurable-intelligent-surface-assisted B5G/6G wireless communications: Challenges, solution, and future opportunities," *IEEE Commun. Mag.*, vol. 61, no. 1, pp. 16–22, 2023.
- [5] A. Mukherjee, V. Kumar, and L.-N. Tran, "Secrecy rate maximization for intelligent reflecting surface assisted MIMOME wiretap channels," in *IEEE MILCOM*, 2021, pp. 261–266.
- [6] A. Mukherjee, V. Kumar, D. W. K. Ng, and L.-N. Tran, "On the energy-efficiency maximization for IRS-assisted MIMOME wiretap channels," in *IEEE VTC (Fall)*, 2022, pp. 1–6.
- [7] H. Du, J. Kang, D. Niyato, J. Zhang, and D. I. Kim, "Reconfigurable intelligent surface-aided joint radar and covert communications: Fundamentals, optimization, and challenges," *IEEE Veh. Technol. Mag.*, vol. 17, no. 3, pp. 54–64, 2022.
- [8] R. Liu *et al.*, "Integrated sensing and communication with reconfigurable intelligent surfaces: Opportunities, applications, and future directions," *IEEE Wireless Commun.*, vol. 30, no. 1, pp. 50–57, 2023.
- [9] X. Song *et al.*, "Joint transmit and reflective beamforming for IRS-assisted integrated sensing and communication," in *IEEE WCNC*, 2022, pp. 189–194.
- [10] H. Luo, R. Liu, M. Li, Y. Liu, and Q. Liu, "Joint beamforming design for RIS-assisted integrated sensing and communication systems," *IEEE Trans. Veh. Technol.*, vol. 71, no. 12, pp. 13 393–13 397, 2022.
- [11] R. Liu, M. Li, and A. L. Swindlehurst, "Joint beamforming and reflection design for RIS-assisted ISAC systems," in *EUSIPCO*, 2022, pp. 997–1001.
- [12] R. P. Sankar and S. P. Chepuri, "Beamforming in hybrid RIS assisted integrated sensing and communication systems," in *EUSIPCO*, 2022, pp. 1082–1086.
- [13] A. A. Salem, M. H. Ismail, and A. S. Ibrahim, "Active reconfigurable intelligent surface-assisted MISO integrated sensing and communication systems for secure operation," *IEEE Trans. Veh. Technol.*, to appear.
- [14] M. Hua, Q. Wu, W. Chen, O. A. Dobre, and A. L. Swindlehurst, "Secure intelligent reflecting surface aided integrated sensing and communication," *arXiv preprint arXiv:2207.09095*, 2022.
- [15] B. Feng *et al.*, "Optimization techniques in reconfigurable intelligent surface aided networks," *IEEE Wireless Commun.*, vol. 28, no. 6, pp. 87–93, 2021.
- [16] X. Yu *et al.*, "Robust and secure wireless communications via intelligent reflecting surfaces," *IEEE J. Sel. Areas Commun.*, vol. 38, no. 11, pp. 2637–2652, 2020.
- [17] V. Kumar, R. Zhang, M. D. Renzo, and L.-N. Tran, "A novel SCA-based method for beamforming optimization in IRS/RIS-assisted MU-MISO downlink," *IEEE Wireless Commun. Lett.*, vol. 12, no. 2, pp. 297–301, 2023.
- [18] MOSEK ApS, *MOSEK Fusion API for Python. Release 10.0.40*, 2023. [Online]. Available: <http://docs.mosek.com/10.0/pythonfusion.pdf>
- [19] A. Ben-Tal and A. Nemirovski, *Lectures on modern convex optimization*. Philadelphia: SIAM, 2011.